

DIVISION S-1—SOIL PHYSICS

Simultaneous Measurement of Soil Penetration Resistance and Water Content with a Combined Penetrometer–TDR Moisture Probe

Carlos Manoel Pedro Vaz and Jan W. Hopmans*

ABSTRACT

Soil mechanical impedance affects root growth and water flow, and controls nutrient and contaminant transport below the rooting zone. Among the soil parameters affecting soil strength, soil water content and bulk density are the most significant. However, field water content changes both spatially and temporally, limiting the application of cone penetrometers as an indicator of soil strength. Considering the presence of large water content variations within a soil profile and across a field and the large influence of water content on soil strength, there is need for a combined penetrometer–moisture probe to provide simultaneous field water content and soil resistance measurements. Such a probe was developed, which uses the time domain reflectometry (TDR) technique to determine water content and its influence on soil penetration resistance. The coiled TDR moisture probe consists of two parallel copper wires, each 0.8 mm in diameter and 30 cm long, coiled around a 5-cm-long polyvinyl chloride (PVC) core with a 3-mm separation between wires. Calibration curves relating the soil bulk dielectric constant measured by the coiled probe to water content were obtained in the laboratory for a Columbia fine sand loam (coarse-loamy, mixed, superactive, nonacid, thermic Oxyaquic Xerofluvent), a Yolo silt clay loam (fine-silty, mixed, nonacid, thermic Typic Xerorthent), and washed sand, and data were analyzed based on a mixing model approach. Subsequently, field experiments were conducted to measure simultaneously the penetration resistance (PR) and water content along a soil profile. Results showed a detailed water content profile with excellent correlation with the gravimetric method, whereas the depth distribution of PR was similar to that of dry bulk density as determined from soil cores.

SOIL MECHANICAL STRENGTH is an important soil parameter that affects root growth and water movement and controls nutrient and contaminant transport below the rooting zone. The most common way to assess soil strength is by using a soil penetrometer, which characterizes the force needed to drive a cone of specific size into the soil (Bradford, 1986). The measured PR depends on such soil properties as bulk density, water content and potential, texture, aggregation, cementation, and mineralogy.

Soil scientists have related changes in PR as caused by tillage, traffic, or soil genetic pans to root growth, crop yields, and soil physical properties. For example, correlation between PR and crop root growth and water

and nutrient exploration have been obtained (Stelluti et al., 1998), and cone penetrometers have been used extensively in soil science studies to identify natural and induced compacted layers (Henderson, 1989) or to predict related soil properties (Ayers and Bowen, 1987).

Among the soil parameters that affect PR, soil water content and bulk density are the most significant (Vazquez et al., 1991). For example, Stitt et al. (1982) conducted a comprehensive study of factors affecting PR in coarse-textured soils in the Atlantic Coastal Plain, and used stepwise regression to relate mechanical impedance to various measured soil properties. The highest correlation coefficients were found for a regression model that included soil water content, soil particle roughness and bulk soil density. Shaw et al. (1942) concluded that soil moisture is the dominant factor influencing the force required to push a penetrometer into the soil, with PR increasing as the moisture content decreased. In an experimental study by Henderson et al. (1988) it was found that PR was only slightly affected with a decrease of soil water content to $\approx 70\%$ of field capacity. However, the PR increased exponentially with a further reduction of the water content of the sandy soil. This study showed that PR increased with an increase of bulk density across the whole measured water content range. However, because soil moisture varies both spatially and temporally and is only one of the soil variables related to PR, the utility of using PR to determine compaction effects is marginal. Moreover, interpretation of penetrometer data is difficult because water content or density measurements can generally not be taken at the exact same spatial location as the penetration resistance measurement.

Considering the strong dependence of PR on soil water content within a soil profile and across a field, it would be beneficial if both soil water content and soil resistance could be measured simultaneously at the same location and depth with a single probe. Among available techniques for soil water content measurements, TDR is the most attractive. Advantages of TDR over other soil water content measurement techniques include (i) potential for variable measurement volume size using different probe sizes and geometry, (ii) the use of the same probe for both laboratory and field measurements, (iii) small influence of dissolved solutes on the TDR moisture measurement within a low salinity range, (iv) its potential for automatic data acquisition

C.M.P. Vaz, EMBRAPA, Agricultural Instrumentation, P.O. Box 741, Sao Carlos-SP, 13560-970, Brazil; J.W. Hopmans, Department of Land, Air and Water Resources, Hydrology Program, 123 Veihmeyer Hall, University of California, Davis, CA 95616. Received 24 Sept. 1999. *Corresponding author (jwhopmans@ucdavis.edu).

Abbreviations: PR, penetration resistance; PVC, polyvinyl chloride; TDR, time domain reflectometry.

and multiplexing, and (v) that it does not pose a radiation hazard.

Most commercial TDR equipment uses standard waveguides or probes with a usual length of 15 to 30 cm. The soil water content value is obtained from calibration curves using the travel time of an electromagnetic wave along the waveguide to determine the bulk dielectric constant of the soil (Topp et al., 1980). A minimum probe length is controlled by the rise time of the electromagnetic square wave reflected at the beginning and end of the TDR probe (Nissen et al., 1998). Petersen et al. (1995) examined the importance of probe length and diameter, distance between wave guides, and horizontal installation depth. They obtained excellent waveforms using a 5-cm probe in a coarse sandy soil with a water content of $0.21 \text{ cm}^3 \text{ cm}^{-3}$. Kelly et al. (1995) obtained an accuracy of $0.035 \text{ cm}^3 \text{ cm}^{-3}$ using TDR probes as short as 2.5 cm and a high-band width TDR system of 20 MHz. Amato and Ritchie (1995) experimented with short probes ranging in length from 1 to 15 cm. They concluded that at water content values of $0.07 \text{ cm}^3 \text{ cm}^{-3}$ with travel times larger than 100 ps, the error in the water content was less than three volume percent. However, for water content measurements in drier soils with shorter travel times, errors were larger than 4 to 5%. Malicki et al. (1992) and Sri Ranjan and Domytrak (1997) described successfully the use of TDR mini-probes (5 cm long) for a clay loam soil.

Selker et al. (1993) introduced a serpentine type surface probe (10 by 10 cm) by imbedding the conductor and ground wires of the TDR probe within an acrylic plate, enabling miniaturization of TDR probes for high spatial resolution measurements. For the coiled probe developed by Nissen et al. (1998) the conductor wire

was guided around a cylindrical PVC rod with four straight ground wires along the PVC rod. Their TDR probe allowed a reduction in probe length of a factor of five without a loss in sensitivity. To avoid short-circuiting, the conductor and ground wires were lacquer-coated. In both designs, the increased conductor wire lengths ensured long enough travel times for accurate water content measurements despite the smaller measured bulk soil volume. Both designs (serpentine and coil) are innovative compared with the traditional two, three, or four rod probes and bring many new TDR applications.

The concept of a combined measurement of penetration resistance and water content was previously presented (Ward, 1994; Young et al., 1998; Adams et al., 1998; Newman and Hummel, 1999; Vaz et al., 1999), but to date details regarding construction and calibration for different soils has been limited. For that reason, the objective of this work was to design, construct, and evaluate a coiled TDR probe to be used in combination with a cone penetrometer to determine water content and penetration resistance along a soil profile in a field setting. After analysis of the testing in the laboratory, the combined penetrometer-TDR soil moisture probe measurement results for the field are presented.

MATERIALS AND METHODS

Coiled and Conventional TDR Probe Design

The presented coiled TDR probe combines the advantages of both the coil (Nissen et al., 1998) and serpentine (Selker et al., 1993) designs, with the TDR integrated into the cone penetrometer. The basic configuration of this coiled probe (Fig. 1a and 1b) consists of two parallel copper wires (ground

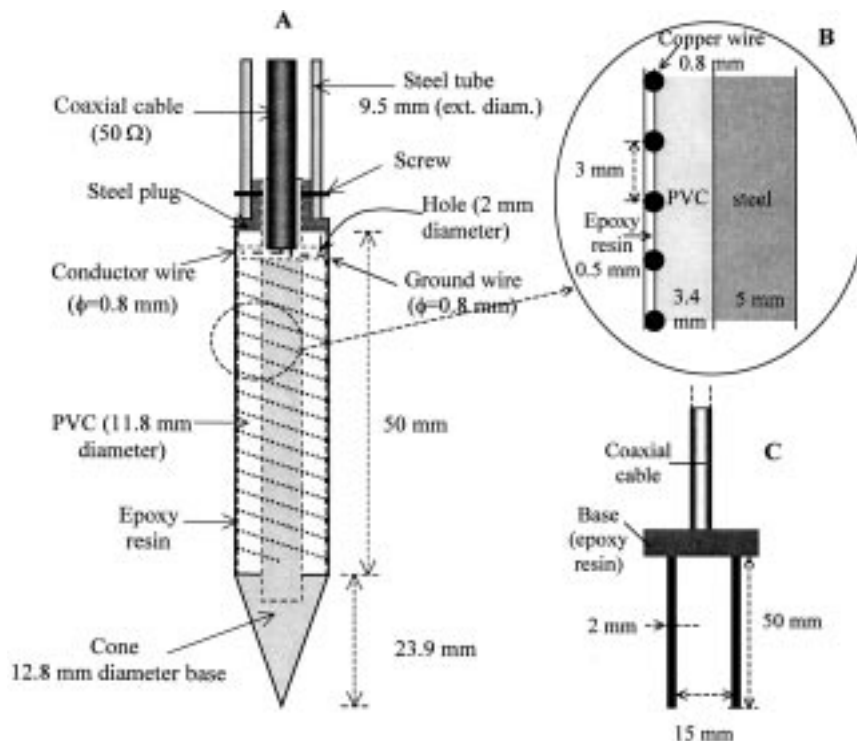


Fig. 1. Detailed (A) diagram and (B) a cross section of the coiled time domain reflectometry (TDR) and (C) the conventional TDR probe.

and conductor wire), each 0.8 mm in diameter and 30 cm long, coiled around a 5-cm-long PVC core, with a 3-mm separation distance between the two wires. The coil is constructed at the bottom of the penetrometer rod, immediately above the cone of the penetrometer. A 2.5-m-long 50 Ω coaxial cable is passed through the hollow steel shaft of the penetrometer probe and connected to a cable tester (Tektronix 1502C, Tektronix, Beaverton, OR). Both copper wires were soldered to the corresponding conductor and ground of the coaxial cable in two opposing 2-mm access holes, right above the coil, as shown in Fig. 1a. The spaces between the wires of the coil and the two access holes were filled with an epoxy resin (2-Ton crystal clear epoxy, Devcon, Riviera Beach, FL) and smoothed to avoid the creation of air spaces between the wires during soil insertion. However, probe-soil contact is also largely affected by the probe operator as straight vertical insertion is required. Figure 2 shows the details of the combined TDR-cone penetrometer probe.

A 5-cm-long conventional TDR probe (illustrated in Fig. 1c) was constructed to independently measure the bulk soil dielectric constant of soil cores used in the calibration of the coiled probe. The two parallel brass rods (2-mm diam. and 15 mm apart) were soldered directly to a 50 Ω coaxial cable mounted in an epoxy resin base as shown in Fig. 1c.

Laboratory Calibration

The waveform or trace is transferred from the cable tester to a personal computer through the RS232 serial port and

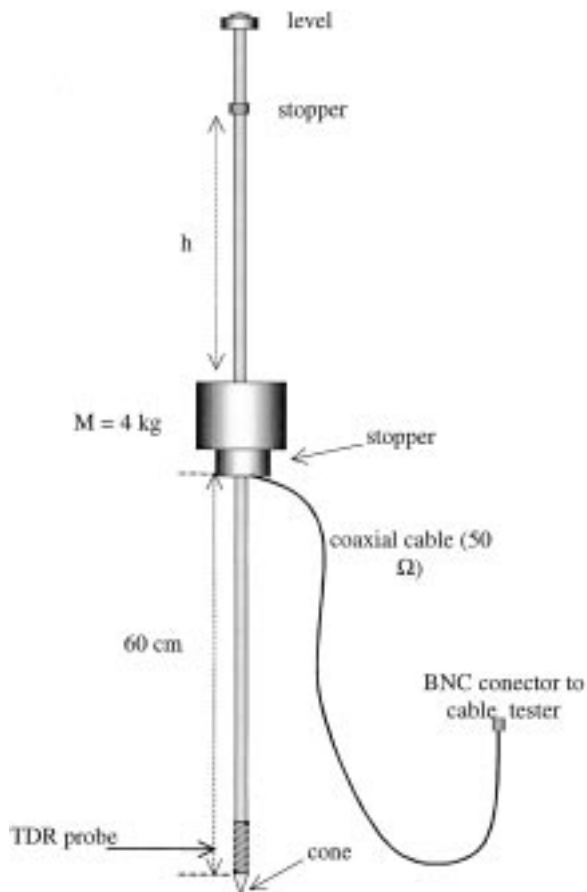


Fig. 2. Combined coiled time domain reflectometry (TDR)-cone penetrometer probe.

analyzed. The trace (Fig. 3a and 3b) is a visualization of the amplitude of a reflected pulsed electromagnetic wave as a function of propagation or travel time along the TDR probe. The trace can be regarded as a signature of the physical status of the soil, and it can be shown that knowledge of the travel time is sufficient to determine the bulk material dielectric constant of the soil (Topp et al., 1980). Travel times and bulk dielectric constant are determined by identification of the first and second reflection at the beginning and end of both TDR probe types. The procedural steps used to identify these reflec-

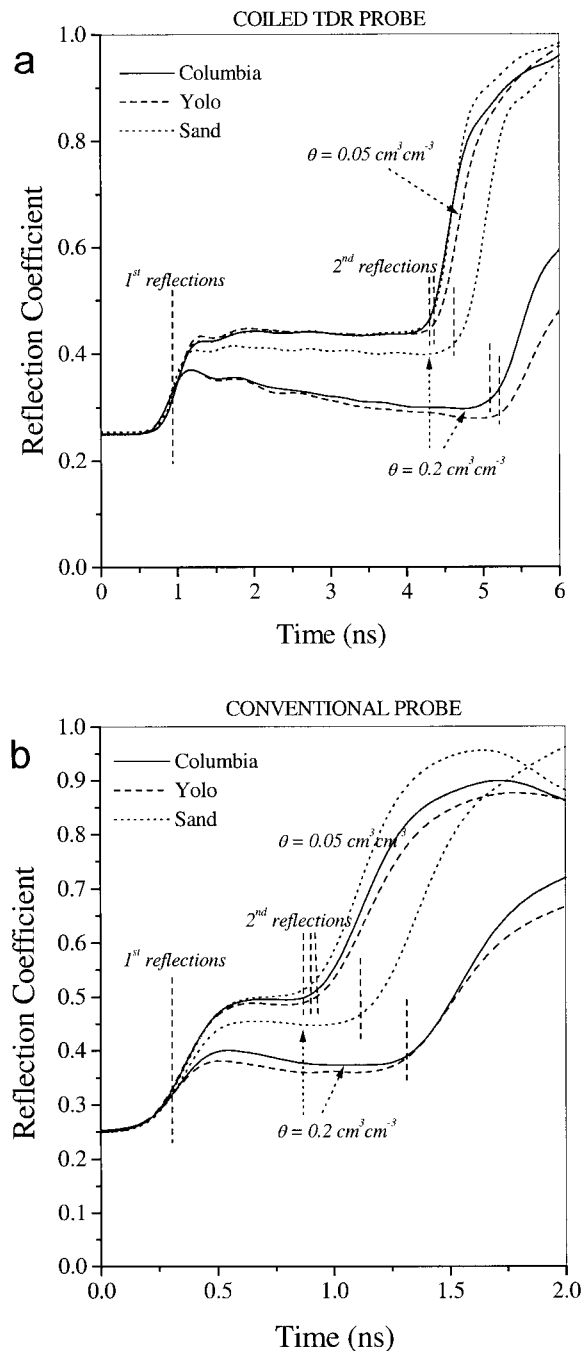


Fig. 3. Representative waveforms for the (a) coiled time domain reflectometry (TDR) and (b) conventional probe designs for the three investigated soil materials at water contents values of 0.05 and 0.20 cm³ cm⁻³. Vertical lines mark the first and second reflection points.

tion points were (i) smoothing of the waveform using a moving average approach and (ii) computation of the first and second time-derivatives of the smoothed waveform. Electric shorting of the probe at its beginning and end was used to confirm correct identification of the beginning and end reflection points of the TDR probes (Hook et al., 1992; Kelly et al., 1995; Nissen et al., 1998). Since the dielectric constant measured by the combined probe is a weighted average dielectric constant of the soil and the PVC and epoxy material between the TDR wires, a conventional TDR probe with two parallel wave guides of 5-cm length was used (Fig. 1c) to estimate the bulk soil dielectric constant of the investigated soil samples (ϵ_{soil}). Using the mixing model approach of Nissen et al. (1998), the dielectric constant measured by the coiled TDR probe (ϵ_{coil}) can be related to the soil dielectric constant as determined by the conventional probe (ϵ_{soil})

$$\epsilon_{\text{coil}} = [w\epsilon_{\text{probe}}^n + (1 - w)\epsilon_{\text{soil}}^n]^{1/n} \quad [1]$$

In Eq. [1], w is a weighting factor that partitions the measured dielectric by the coiled TDR probe between contributions by the epoxy and PVC of the probe (ϵ_{probe}) and the bulk soil (ϵ_{soil}). An optimal design of the coiled probe would minimize the contribution of the probe to the dielectric measurement (or minimize the value of w), thereby maximizing the sensitivity of the coiled probe measurement to bulk soil water content. The parameter n defines the probe's geometry, and ϵ_{probe} is the dielectric constant of the PVC and epoxy material in which the wire coils are imbedded. The dielectric constant of the soil (ϵ_{soil}) as determined by the conventional two-rod probe is written in terms of the fractional bulk volume of each of the three soil phases ($1 - \phi$, $\phi - \theta$, and θ , for the solid, gas, and water phase, respectively), according to Dobson et al. (1985)

$$\epsilon_{\text{soil}} = [(1 - \phi)\epsilon_s^\alpha + (\phi - \theta)\epsilon_a^\alpha + \theta\epsilon_w^\alpha]^{1/\alpha} \quad [2]$$

where ϕ ($\text{cm}^3 \text{cm}^{-3}$) and θ ($\text{cm}^3 \text{cm}^{-3}$) denote the soil porosity and volumetric water content, respectively, and ϵ_s , ϵ_a , and ϵ_w are the dielectric constant of the soil solid material, air, and water, respectively, with assumed values of $\epsilon_s = 1.0$; $\epsilon_w = 80$, and $\epsilon_s = 3.9$ (Dasberg and Hopmans, 1992). The ϵ_s value varies slightly with mineralogical composition of the soil solid material (Yu et al., 1999). For instance, the dielectric constant of quartz can vary between 3.75 and 4.1 (Lide, 1996), whereas an Al silicate has a dielectric constant of 4.8 (Fink, 1978). Also, the presence of organic matter increases the dielectric constant of organic soils to values as high as 5.0. For the mineral soils studied here, an ϵ_s value of 3.9 appears to be a good estimation for the investigated mineral soils. The exponent α depends on the geometry of the soil solid phase and the soil's orientation with respect to the applied electric field and must be $-1 < \alpha < +1$ (Roth et al., 1990).

After substitution of Eq. [2] into [1], the dielectric constant as measured with the coiled TDR probe (ϵ_{coil}) can be written as

$$\epsilon_{\text{coil}} = \{w\epsilon_{\text{probe}}^n + (1 - w)[(1 - \phi)\epsilon_s^\alpha + (\phi - \theta)\epsilon_a^\alpha + \theta\epsilon_w^\alpha]^{n/\alpha}\}^{1/n} \quad [3]$$

The presented mixing model approach is preferred to allow for a meaningful physical interpretation of the calibration results (Roth et al., 1990), rather than the model fitting of an arbitrary empirical functional relationship. Moreover, the application of Eq. [3] inherently corrects for the influence of bulk soil density on the bulk soil dielectric constant. Alternatively, one can simply use a polynomial to substitute for Eq. [3], writing ϵ_{coil} as a function of water content, and fit the data

Table 1. Soil characteristics and α values for investigated soils ($n = 0.494$, $w = 0.655$ and $\epsilon_{\text{probe}} = 2.703$).

Soil material	Number of samples	Bulk density		α (Eq. [2])
		Average	SD*	
		— g cm^{-3} —		
Columbia	36	1.457	0.101	0.538
Yolo	24	1.276	0.086	0.554
Sand	29	1.456	0.038	0.320

to estimate the regression coefficients as was done in Topp et al. (1980), and later for the field calibration results.

Three different soil materials were used to test the coiled TDR probe in the laboratory. These soils were a Yolo silt clay loam (Eching et al., 1994), a Columbia fine sandy loam (Liu et al., 1998), and a washed sand (SRI supreme sand-30, Silica Resources, Marysville, CA). Samples with different water content values (range of $0.0\text{--}0.35 \text{ cm}^3 \text{cm}^{-3}$) were obtained after mixing a known amount of water to a fixed amount of dry soil. Wetted soils were packed in brass cores (8.25-cm-i.d., 9 cm high) at approximately constant dry bulk densities (Table 1) by packing a predetermined mass of dry soil into the known core volume. Subsequently, samples were covered to prevent water loss by evaporation and put aside for at least 1 d to allow for water distribution before TDR measurements were taken.

Bulk soil dielectric constants were measured at three different locations in each soil core with both the coiled and the conventional TDR probe. The dielectric constant was first measured with the conventional probe. Subsequently, the combined coiled TDR probe was inserted into the soil by manually pushing the penetrometer rod into the soil, sufficiently away from the holes created by the two-prong TDR probe. The TDR measurements were taken immediately after probe insertion, while assuring that the core wall did not affect travel times. Both probe types were inserted vertically and measurement depth increments for both probes were identical (0–5 cm below the soil core surface). In order to ensure the correct response of both probe types to changes in soil water content, dielectric measurements were conducted in triplicate and subsequently averaged, and utmost care was taken to prevent air spaces between the TDR probes and the surrounding soil. After TDR readings were completed, soil samples were weighed and oven-dried, from which gravimetric volumetric water content and bulk density values were obtained. In the calibration procedure, the average of three replicate TDR measurements was used.

Calibration curves of ϵ_{soil} vs. $\theta_{\text{gravimetric}}$ were obtained with the mixing model described by Eq. [1], [2], and [3] in two steps using the fitting-model software (Wraith and Or, 1998). First, from TDR measurements of the conventional (ϵ_{soil}) and the coiled (ϵ_{coil}) probe for all three soils together and across the whole water content range, values for w , n , and ϵ_{probe} were fitted to Eq. [1] using the fitting-model software. Subsequently, Eq. [2] was fitted for each soil type to estimate soil-specific α values using independent values for porosity (as estimated from the soil core density) and volumetric water content values for each soil core.

Fitted n , w , and ϵ_{probe} and specific α values for Columbia soil, Yolo soil, and sand were used in Eq. [3] to produce the soil-specific calibration curves using average values of bulk density and porosity (considering a soil particle density of 2.6 g cm^{-3}).

Theory of Dynamic Penetrometer Resistance

The cone penetrometer as used in this study (Fig. 2) is classified as an impact-loading or hammer penetrometer,

yielding dynamic penetration characteristics (Bradford, 1986). This type of penetrometer was selected because of its simplicity and ease of construction. Moreover, because soil penetration occurs through several impacts, there is time to measure the water content by the TDR between impacts (≈ 1 min).

During the impact-loading test of the cone penetrometer, the energy stored in the weight at a known elevation is used to drive the penetrometer rod into the soil. The depth of penetration achieved by application of the constant amount of energy is used as a measure of soil PR. The PR can be determined considering that the potential energy of the impact body is converted into work of cone penetration. The total potential energy of the system after impact is equal to the energy of the impact body at height h (m) plus the potential energy of an additional penetration distance x (m). After consideration of the loss of energy due to the impact and the inelastic collision of the weight with the stopper (Fig. 2), we can write (Terzaghi and Peck, 1978; Stolf, 1991)

$$Fx = (Mgh)f + (M + m)gx \quad [4]$$

where F (N) is the force of penetration, x (m) is the penetration distance after one impact, M (kg) and m (kg) are the mass of the impact body and the cone penetrometer system, respectively, and g (m s^{-2}) is the gravitational constant. The left side of Eq. [4] describes the penetration work due to a single impact, whereas the terms on the right side account for the energy available for penetration, a multiplication factor to describe energy loss due to the impact, and the last term describes the potential energy of the penetrometer system after the collision. The energy loss factor, f , is determined by the relation between the kinetic energy of the system immediately before (K_b) and after (K_a) the collision (Eq. [5]) and can be computed using the conservation of linear momentum Eq. [6]

$$f = \frac{K_a}{K_b} = \left(\frac{M + m}{M} \right) \left(\frac{v_a}{v_b} \right)^2 \quad [5]$$

$$Mv_b = (M + m)v_a \quad [6]$$

and yields

$$f = \frac{M}{M + m} \quad [7]$$

The PR is obtained from combination of Eq. [7] and [4], which yields after division of the penetration force, F , by the base area of the cone, A (m^2),

$$\text{PR} = \left(\frac{Mgh}{Ax} \right) \left(\frac{M}{M + m} \right) + \frac{(M + m)g}{A} \quad [8]$$

The characteristics of the penetrometer used in this study (Fig. 2) are $M = 4$ kg, $m = 1.335$ kg, $h = 0.4$ m, $A = 1.287 \times 10^{-4}$ m^2 , and $f = 0.75$. Substituting these data in Eq. [8], we obtain the equation used to determine the PR (MPa) related to the penetration distance x (m).

$$\text{PR} = 0.40624 + \frac{0.09135}{x} \quad [9]$$

Standard penetrometers have a rod diameter slightly smaller than the cone base diameter, to avoid friction between the penetrometer rod and the soil material. However, the combined penetrometer–moisture probe has a rod diameter equal to the cone diameter, to avoid air gaps and to ensure good contact between the coiled probe and soil. Therefore, using Eq. [9] may overestimate penetration resistance, when compared with standard cone penetrometer measurements,

since we neglect friction losses by the coiled TDR section of the penetrometer. Hence, additional work will be needed to quantify the friction effect on PR measurements with the combined probe.

Field Measurements

In addition to the laboratory tests, the coiled penetrometer probe was tested for the Yolo soil at the Campbell Tract experimental field of the University of California at Davis. The soil is a Yolo silty clay loam with an approximate clay content of 21%, with its texture approximately uniform within the top 60 cm. Measurements of PR and water content were carried out to the 60-cm soil depth. After each impact, penetration depth and water content, as calculated by the WinTDR98 software (Soil Physics Group, Utah State University, 1998) were recorded. Time between impacts was ≈ 1 min. After completion of the coil–penetrometer probe measurements, core samples were taken in 5-cm increments from the soil surface to the 60-cm depth using aluminum rings (5-cm diam. and 5-cm height) for subsequent bulk soil density and gravimetric water content determinations in the laboratory. To improve data interpretation, we will present the penetration resistance and the water content profile data combined in a single graph, using depth-average values along 5-cm depth intervals.

RESULTS AND DISCUSSION

Laboratory Measurements

Figures 3a and 3b show the waveforms obtained with the coiled and the conventional TDR probe for all three soils as measured from soil cores with independently measured core-average volumetric water content values of 0.05 and 0.20 $\text{cm}^3 \text{cm}^{-3}$. Water contents were determined from the travel times of each electromagnetic wave as calculated from the difference in travel time between the first and second reflection. As expected, this travel time is much higher for the coiled probe than the conventional TDR probe (Table 2), since the coiled wire is much longer than the straight wire of the conventional probe (30 vs. 5 cm). Therefore, as pointed out by Nissen et al. (1998) and Selker et al. (1993), the sensitivity of the coiled TDR probe has increased. As would be expected, the waveforms in Fig. 3 also demonstrate that the bulk soil travel time increases as the soil water content and bulk soil dielectric constant increase.

The experimental relation between the dielectric constant measured by the coiled TDR probe (ϵ_{coil}) and the conventional probe (ϵ_{soil}), using the data of all three soils is shown in Fig. 4. The apparent outliers for the sandy material for ϵ_{coil} values larger than 4.5 may be caused by inadequate probe–soil contact of the coiled probe

Table 2. Travel times calculated from waveforms presented in Fig. 3.

Soil type	Travel time			
	$\theta = 0.05 \text{ cm}^3 \text{ cm}^{-3}$		$\theta = 0.20 \text{ cm}^3 \text{ cm}^{-3}$	
	Coiled	Conventional	Coiled	Conventional
	ns			
Columbia	3.34	0.59	4.16	1.01
Yolo	3.42	0.63	4.29	1.01
Sand	3.33	0.57	3.68	0.81

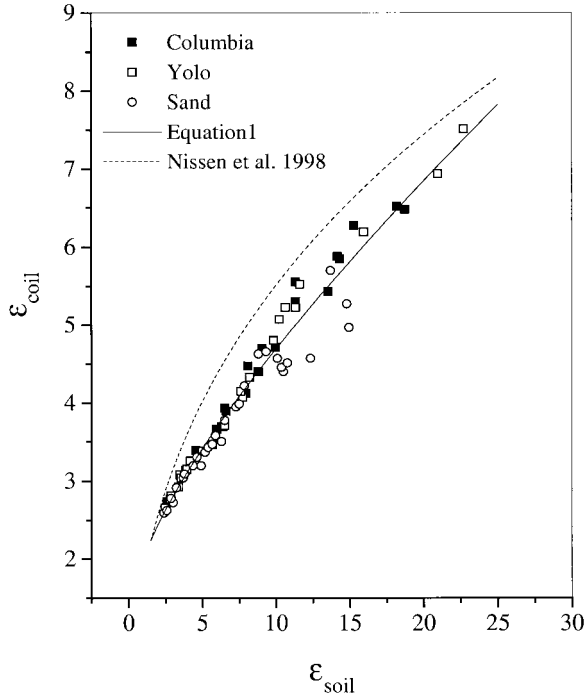


Fig. 4. Relationship between dielectric constant as measured by the coiled (ϵ_{coil}) and conventional (ϵ_{soil}) time domain reflectometry (TDR) probes for investigated soils.

for that soil. Using model-fitting software (Wraith and Or, 1998), data were fitted to Eq. [1] yielding parameter values of $n = 0.494$, $w = 0.655$, and $\epsilon_{probe} = 2.703$. A w value of 0.655 indicates the large influence of the probe material on the dielectric measurement for the coiled TDR probe. Possibly, the geometry of the coiled probe can be changed (wire thickness and spacing and epoxy thickness) to reduce this w value, thereby increasing the

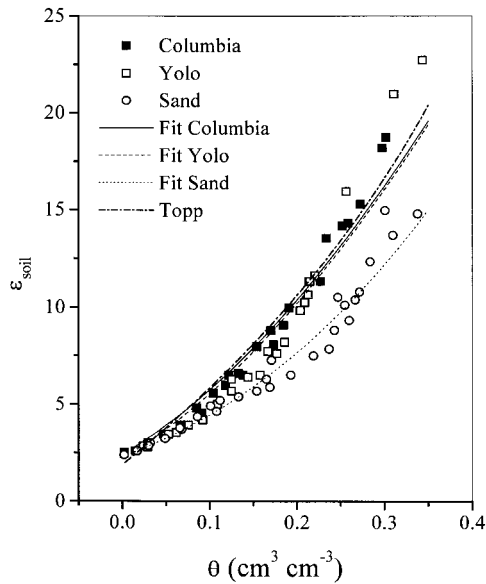


Fig. 5. Calibration data for the conventional time domain reflectometry (TDR) probe, using Eq. [2] for all three soil types (from average values of bulk density and porosity in Table 1), and compared with Topp's (1980) model. Range in water content is identical to that in Fig. 4 and 6.

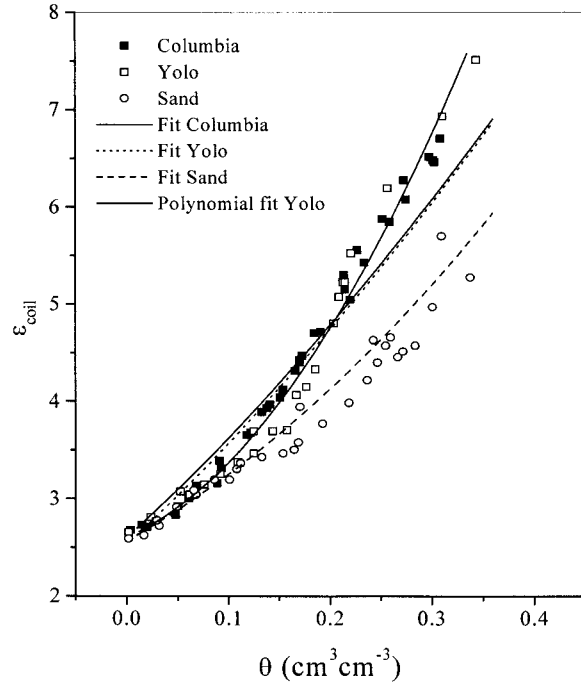


Fig. 6. Calibration data for the coiled TDR probe using Eq. [3] for all three soil types (from average values of bulk density and porosity in Table 1), using parameters n , w , ϵ_{probe} fitted to Eq. [1] and soil specific α values fitted to Eq. [2]. Fitted polynomial ($\theta = -0.2977 + 0.1443\epsilon_{coil} - 0.00824\epsilon_{coil}^2$; $r^2 = 0.963$) is used for field measurements.

sensitivity of the coiled TDR probe. The fitted ϵ_{probe} value of 2.703 is sufficiently close to handbook values of PVC or epoxy of 3.3 and 3.6, respectively (Weast, 1982), thereby validating the parameter fitting approach to some extent. For their specific TDR probe, Nissen et al. (1998) determined a w value of 0.52 and an n value of -0.13 , and their fitted relationship is included in Fig. 4 for comparative purposes. Differences in w and n parameters are caused by specific probe characteristics. As expected, there is a nonlinear relationship between the coiled and the conventional probe caused by the constant contribution of the probe material (see Eq. [1]) to the coiled probe (Nissen et al., 1998).

The parameter α was calculated by fitting Eq. [2] to the experimental data obtained with the conventional probe (Fig. 5) using the model-fitting software and core specific values of porosity and water content. Fitted α values obtained were 0.538, 0.554, and 0.320 for the Columbia soil, the Yolo soil, and the sand, respectively (Table 1). The α values found for the Columbia and Yolo soil were relatively close to reported values of about 0.5 for various soils (Dobson et al., 1995; Dasberg and Hopmans, 1992; Roth et al., 1992; Panizovsky et al., 1999). However, the low α value found for the sand can be attributed to inadequate soil-probe contact of the two-rod conventional probe as well, thereby causing deviations from the generally accepted Topp equation (Walley, 1993), which is also presented in Fig. 5.

The calibration data of the coiled TDR probe for all three soils are presented in Fig. 6. Calibration curves (lines in Fig. 6) for the coiled probe were obtained substituting the fitted parameters n , w , and α (for each

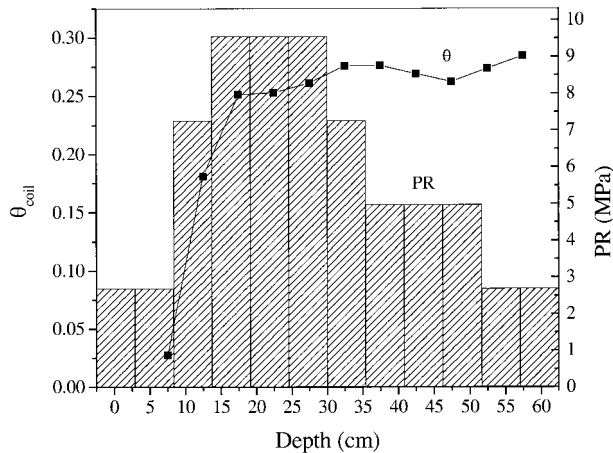


Fig. 7. Combined field measurement results of penetration resistance (PR) and water content (θ) obtained with the combined coiled time domain reflectometry (TDR)-cone penetrometer probe for the Yolo soil.

soil) in Eq. [3] and using average values of bulk density and porosity (considering soil particle density equal 2.6 g cm^{-3}) presented in Table 1. Alternatively, as indicated earlier, rather than using the physically based approach presented, the data of Fig. 6 can be fitted directly to an empirical model, thereby circumventing the need for bulk soil dielectric measurements by the conventional two-prong TDR probe. The results in Fig. 5 and 6 show that the dielectric constant values for all soils are close in the water content range of 0.0 to $0.10 \text{ cm}^3 \text{ cm}^{-3}$ for both conventional and coiled probes. However, as the water content further increases, the bulk dielectric constant of the sand is increasingly lower than for the other two soils, despite its higher bulk density compared with the Yolo soil. In a glance, quite the opposite would be expected, since a larger soil density (Table 1) will increase the bulk dielectric constant (Dirksen and Dasberg, 1993), whereas the presence of possible bound water in the finer-textured soil (Columbia and Yolo) may decrease the bulk soil dielectric constant in those soils (Dasberg and Hopmans, 1992).

There are two aspects for consideration to better understand the calibration results of both probes (Fig. 5 and 6). The first aspect is the displacement of the sandy soil material around the probe during probe insertion. It was visually observed that the sandy material was displaced at the soil sample surface. The soil displacement created air spaces between the probe and the surrounding sand material, thereby resulting in low dielectric values (Knight et al., 1997) for both probes (Fig. 5 and 6), relative to the other two soil types. Displacement of the sand was more apparent for the coiled than the conventional TDR probe. The second aspect to be considered is the apparent soil compaction in the radial direction by probe insertion for the Columbia and Yolo soil. The compaction probably caused a slight increase in soil bulk density and water content in the immediate vicinity of the TDR probes. Compaction is expected to be more significant for the coiled probe because of its larger volume. According to Roth et al. (1997), who quantified the compaction effect using x-ray computed

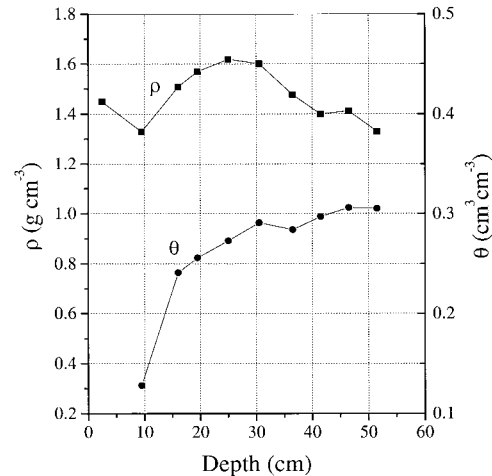


Fig. 8. Independent values for dry soil bulk density and water content for the Yolo soil in the field, determined from gravimetric measurements of soil core samples collected at the same plot of the combined penetrometer-coiled time domain reflectometry (TDR) probe measurements.

tomography, soil compaction caused by probe installation can increase the soil bulk dielectric constant, depending on soil type, rod diameter, and soil water content at the moment of probe installation. Although soil density changes by compaction appear significant only within a relatively small soil volume around the probe, it is expected that the travel time of the electromagnetic wave will be affected, since measurement volumes of the TDR signal are small as well (Nissen et al., 1998). Also, we conducted laboratory experiments to directly measure soil density changes in soil cores, from soil sampling around the TDR probe. However, although soil compaction was observed, the large measurement error of soil density due to small sample volumes deemed these results to be uncertain.

Hence, we postulate that differences in α values and calibration curves (Fig. 6) between soils are caused by compaction (Columbia and Yolo) and displacement (sand) of soil material in the immediate vicinity of the TDR probe during probe insertion. Possible compaction of the Columbia and Yolo soil near the probe will cause an increment in the soil bulk dielectric as measured by TDR, whereas displacement of the sandy material by the probe creates air spaces between the TDR probe and surrounding soil, thereby decreasing the soil bulk dielectric constant (Ferre et al., 1996).

Field Measurements

Volumetric water content and PR measurements with the combined probe were conducted in a bare field research plot with the Yolo soil. Using the combined penetrometer-TDR coiled probe (Fig. 2) in the field required fast data acquisition and processing in order to accurately measure the water content and the penetration resistance simultaneously. For that reason we used the WinTDR software for water content determination. However, the software could not include the mixing model as the calibration curve. Instead, we used

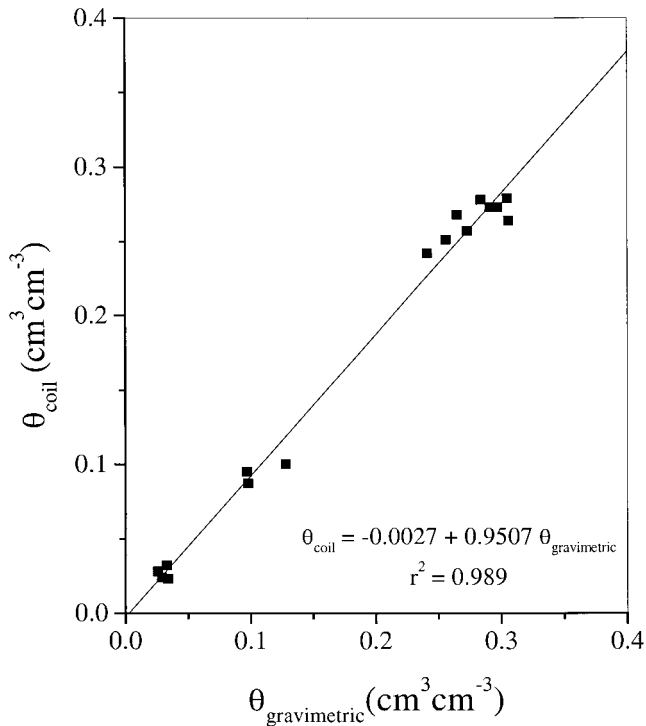


Fig. 9. Correlation between water content measured by the coiled time domain reflectometry (TDR) probe (θ_{coil}) and gravimetric data from collected soil cores for the Yolo field soil.

a second-order polynomial equation ($\theta = -0.2977 + 0.1443\epsilon_{\text{coil}} - 0.00824\epsilon_{\text{coil}}^2$; $r^2 = 0.963$) to fit the field calibration data of the Yolo soil (see also Fig. 6).

Figure 7 shows the results of the field measurements using the combined probe, including both the water content and PR data as a function of soil depth in a single graph. The PR and water content values were determined after each hammer impact and were averaged for each 5-cm depth increment. For example, the high PR for the 15- to 20-cm depth increment required five hammer drops, and hence the water content data were averaged for each 5-cm depth increment, enabling comparison with gravimetric water content data (Fig. 8).

As Fig. 7 shows, the volumetric water content is low near the soil surface and increases with soil depth, whereas the PR increases from the surface to about the 30-cm depth (plough pan) and decreases from there on. Independent water content and bulk density values from extracted soil cores for the same soil profile as for which the combined probe measurements were taken are presented in Fig. 8. Clearly, the measured depth distribution of PR in Fig. 7 follows a similar spatial pattern with depth as the independently measured soil density profile in Fig. 8. However, the water content will affect PR as well. In a followup study it is planned to use the combined penetrometer-coiled TDR probe to quantify and model the influence of the water content and bulk density on penetration resistance. Finally, comparison of gravimetric water content with measurements obtained using the newly developed coiled TDR probe for the Yolo soil shows (Fig. 9) that there is excellent agreement between the two measurements ($r^2 = 0.989$), indicating

that the laboratory calibration can be used satisfactorily for the field measurements.

CONCLUSIONS

According to the results presented, we conclude that the combined coiled TDR-cone penetrometer probe provides accurate water content and soil penetration resistance measurements. The laboratory calibration was successfully used for field measurements in the same soil. The relation between the dielectric constant measured by the coiled TDR probe and bulk soil water content was described well by a dielectric mixing model including dielectric values of the TDR probe material and the bulk soil. Further investigations are needed to better understand the effect of compaction of the cone penetrometer probe on the TDR measurement and the contribution of friction to the penetrometer resistance measurements.

Although it is shown that the concept of the combined penetrometer-coiled TDR probe is valid, it is recommended that alternative TDR designs are considered to increase TDR probe sensitivity to bulk soil water content, while simultaneously conducting additional tests to better define the size of the measurement volume of the coiled TDR probe. Moreover, additional field testing may be needed to determine whether soil-specific calibration is needed or that a single calibration may be used for a range of field soils. Finally, we conclude that the combined penetrometer-TDR moisture probe can be an excellent tool to investigate the water content dependence of soil resistance in field soils.

ACKNOWLEDGMENTS

The authors thank FAPESP (98/04740-7), EMBRAPA, and U.C. Davis for the financial support and Daniel Serrarens, Luis Bassoi, Jim MacIntyre, Atac Tuli, Dennis Rolston, David Page, and Paulo Herrmann for suggestions, discussions, and assistance in the development of the coiled TDR probe. We also acknowledge the thorough reviews by four anonymous reviewers and the associate editor. Their in-depth, critical comments were crucial in the development of the revised manuscript.

REFERENCES

- Adams, B.A., B.D. Young, and G.C. Topp. 1998. Simultaneous measurement of soil resistance and water content. p. 181. In *Agronomy abstracts*. ASA, CSSA, and SSSA, Madison, WI.
- Amato, M., and J.T. Ritchie. 1995. Small spatial scale soil water content measurement with time-domain reflectometry. *Soil Sci. Soc. Am. J.* 59:325-329.
- American Society of Agricultural Engineers. 1994. ASAE standards engineering practices data (Soil cone penetrometer, S313.2). ASAE, St. Joseph, MI.
- Ayers, P.D., and H.D. Bowen. 1987. Predicting soil density using cone penetration resistance and moisture profile. *ASAE Trans.* 30: 1331-1336.
- Bradford, J.L. 1986. Penetrability. p. 463-478. In A. Klute (ed.) *Methods of soil analysis*. Part 1. 2nd ed. Agron. Monogr. 9. ASA and SSSA, Madison, WI.
- Dasberg, S., and J.W. Hopmans. 1992. Time domain reflectometry calibration for uniformly and nonuniformly wetted sandy and clayey loam soils. *Soil Sci. Soc. Am. J.* 56:1341-1345.
- Dirksen, C., and S. Dasberg. 1993. Improved calibration of time do-

- main reflectometry soil water content measurements. *Soil Sci. Soc. Am. J.* 57:660–667.
- Dobson, M.C., F.T. Ulaby, M.T. Hallikainen, and M.A. El-Rayes. 1985. Microwave dielectric behavior of wet soil: II. Dielectric mixing models. *IEEE Trans. Geosci. Remote Sensing* GE-23:35–46.
- Eching, S.O., J.W. Hopmans, and O. Wendroth. 1994. Unsaturated hydraulic conductivity from transient multistep outflow and soil water pressure data. *Soil Sci. Soc. Am. J.* 58:687–695.
- Ferre, P.A., and D.L. Rudolph. 1996. Spatial averaging of water content by time domain reflectometry: Implications for twin rod probes and without dielectric coatings. *Water Resour. Res.* 32:271–279.
- Fink, D.G. 1978. *Standard handbook for electrical engineers*. 11th ed. McGraw Hill, New York.
- Henderson, C.W.L. 1989. Using a penetrometer to predict the effects of soil compaction on the growth and yield of wheat on uniform, sandy soils. *Aust. J. Agric. Res.* 40:498–508.
- Henderson, C., A. Levett, and D. Lisle. 1988. The effects of soil water content and bulk density on the compactibility of some western Australian sandy soils. *Aust. J. Soil Res.* 26:391–400.
- Hook, W.R., N.J. Livingston, Z.J. Sun, and P.B. Hook. 1992. Remote diode shorting improves measurement of soil water by time domain reflectometry. *Soil Sci. Soc. Am. J.* 56:1384–1391.
- Kelly, S.F., J.S. Selker, and J.L. Green. 1995. Using short soil moisture probes with high-bandwidth time domain reflectometry instruments. *Soil Sci. Soc. Am. J.* 59:97–102.
- Knight, J.H., P.A. Ferre, D.L. Rudolph, and R.G. Kachanoski. 1997. A numerical analysis of the effects of coatings and gaps upon relative dielectric permittivity measurement with time domain reflectometry. *Water Resour. Res.* 33:1455–1460.
- Lide, D.R. 1996. *CRC handbook of chemistry and physics*. 77th ed. CRC Press, Boca Raton, FL.
- Liu, Y.P., J.W. Hopmans, M.E. Grismer, and J.Y. Chen. 1998. Direct estimation of air-oil and oil-water capillary pressure and permeability relates from multi-step outflow experiments. *Contam. Hydrol.* 32:223–245.
- Malicki, M.A., R. Plagge, M. Render, and R.T. Walczak. 1992. Application of time-domain reflectometry (TDR) soil moisture mini-probe for the determination of unsaturated soil water characteristics from undisturbed soil cores. *Irrig. Sci.* 13:65–72.
- Newman, S.C., and J.W. Hummel. 1999. Soil penetration resistance with moisture correction. Paper no. 993028, p. 21. *In* ASAE/CSAE/SCGR Annual International Meeting. Toronto, ON, Canada. 18–21 July 1999. ASAE, St. Joseph, MI.
- Nissen, H.H., P. Moldrup, K. Henriksen. 1998. High-resolution time domain reflectometry coil probe for measuring soil water content. *Soil Sci. Soc. Am. J.* 62:1203–1211.
- Panizovsky, A.A., S.M. Chudinova, Y.A. Pachepsky. 1999. Performance of TDR calibration models as affected by soil texture. *J. Hydrol.* 218:35–43.
- Petersen, L.W., P. Tomsen, P. Moldrup, O.H. Jacobsen, and D.E. Rolston. 1995. High resolution time domain reflectometry: Sensitivity dependency on probe design. *Soil Sci.* 159:149–154.
- Roth, A., W. Weis, D. Matthies, U. Hess, and B. Ansoerge. 1997. Changes in soil structure caused by the insertion of time domain reflectometry probes and their influence on the measurement of soil moisture. *Water Resour. Res.* 33:1585–1593.
- Roth, K., M.A. Malicki, and R. Lagge. 1992. Empirical evaluation of relationship between soil dielectric constant and volumetric water content as the basis for calibrating soil moisture measurement by TDR. *J. Soil Sci.* 43:1–13.
- Roth, K., R. Schulin, H. Fluehler, and W. Attinger. 1990. Calibration of TDR for water content measurement using a composite dielectric approach. *Water Resour. Res.* 26:2267–2273.
- Selker, J.S., L. Graff, and T. Steenhuis. 1993. Noninvasive time domain reflectometry moisture measurement probe. *Soil Sci. Soc. Am. J.* 57:934–936.
- Shaw, B.J., H.R. Haise, and R.B. Farnsworth. 1942. Four years experience with a soil penetrometer. *Soil Sci. Soc. Am. Proc.* 7:48–55.
- Soil Physics Group, Utah State University. 1998. WinTDR '98. Available at <http://psb.usu.edu/wintdr99/index.html> (verified 7 Aug. 1999).
- Sry Ranjan, R., and C.J. Domytrak. 1997. Effective volume measured by TDR miniprobos. *Trans. ASAE* 40:1059–1066.
- Stelluti, M., M. Maiorana, and D. DeGiorgio. 1998. Multivariate approach to evaluate the penetrometer resistance in different tillage systems. *Soil Tillage Res.* 46:145–151.
- Stitt, R.E., D.K. Cassel, S.B. Weed, L.A. Nelson. 1982. Mechanical impedance of tillage pans in Atlantic Coastal Plain soils and relationships with soil physical, chemical, and mineralogical properties. *Soil Sci. Soc. Am. J.* 46:100–106.
- Stolf, R. 1991. Teoria e teste experimental de fórmulas de transformação dos dados de penetrômetro de impacto em resistência do solo. *R. bras. Ci. Solo* 15:229–235.
- Terzaghi, K., and R.B. Peck. 1978. *Soil mechanics in engineering practice*. John Wiley and Sons, New York.
- Topp, G.C., J.L. Davis, and A.P. Annan. 1980. Eletromagnetic determination of soil water content: Measurements in coaxial transmission lines. *Water Resour. Res.* 16:574–582.
- Vaz, C.M.P., J.W. Hopmans, and P.S.P. Herrmann. 1999. Development of time domain reflectometry probes for combined use with a cone penetrometer. *In* A. Kraszewski and K.C. Lawrence (ed.) *Workshop on Electromagnetic Wave Interaction with Water and Moist Substances*. Athens, GA. 11–13 Apr. 1999. USDA ARS, Athens, GA.
- Vazques, L., D.L. Myhre, E.A. Hanlon, and R.N. Gallaher. 1991. Soil penetrometer resistance and bulk density relationships after long-term no tillage. *Commun. Plant Anal.* 22:2101–2117.
- Walley, W.R. 1993. Considerations on the use of time-domain reflectometry (TDR) for measuring soil water content. *J. Soil Sci.* 44:1–9.
- Ward, A.L. 1994. Design and optimization of a time domain reflectometry (TDR) based sensor of in situ measurements of soil water content with a site characterization and analysis penetrometer system (SCAPS). N47408-95-D-0730/0040. Pacific Northwest National Lab., Richland, WA.
- Weast, R.C. 1982. *Handbook of physics and chemistry*. 63th ed. CRC Press, Boca Raton, FL.
- Wraith, J.M., and D. Or. 1998. Nonlinear parameter estimation using spreadsheet software. *J. Nat. Resour. Life Sci. Educ.* 27:13–19.
- Young, G.D., B.A. Adams, and G.C. Topp. 1998. A portable cone index and water content penetrometer. p. 180. *In* *Agronomy abstracts*. ASA, CSSA, and SSSA, Madison, WI.
- Yu, C., W. Warrick, and M.H. Conklin. 1999. Derived functions of time domain reflectometry for soil moisture measurements. *Water Resour. Res.* 35:1789–1796.